Synthesis of branched Au nanoparticles with tunable near-infrared LSPR using a zwitterionic surfactant†

P. Pallavicini,*[a] G. Chirico,[b] M. Collini,[b] G. Dacarro,[a] A. Donà,[a] L. D'Alfonso,[b] A. Falqui,[c] Y. Diaz-Fernandez,[a] S. Freddi,[b] B. Garofalo,[a] A. Genovese,[c] L. Sironi[b] and A. Taglietti[a]

Received 20th July 2010, Accepted 27th October 2010
DOI: 10.1039/c0cc02682d

Asymmetric branched gold nanoparticles are obtained using for the first time in the seed-growth approach a zwitterionic surfactant, laurylsulfobetaine, whose concentration in the growth solution allows to control both the length to base-width ratio of the branches and the LSPR position, that can be tuned in the 700–1100 nm near infrared range.

Non spherical gold nano-objects have localized surface plasmon resonance (LSPR) that in many cases falls in the near-infrared region (750–1300 nm),[1] where tissues, blood and water display high transmission of electromagnetic radiation.

This has prompted to propose nanorods (NR) for therapeutic and diagnostic biomedical applications.[2] Beside nanorods, other low symmetry nano-objects, like nanostars[3a–c] and more generally branched nanoparticles (NPs),[3d–j] have been reported to display such optical features. The syntheses of nanostars and branched NPs rely on the seed/growth concept originally elaborated for NR. In the wet synthesis of the latter, spherical gold nano-seeds are added to a growth solution of an Au(III) complex in the presence of a mild reductant and in most cases a surfactant,[4] cetyl trimethylammonium bromide (CTAB).

The CTAB role has been hypothesized to be the preferential coating of the {100} face of the crystalline gold seed,[5] thus protecting it and allowing the anisotropic growth of the nano-object by Au(0) deposition on the {111} face. In the syntheses using CTAB, a major role is also played by Ag^+ that must be present in low but significant concentrations to obtain high aspect ratios (AR = ratio of the long to short axis of a NR).[4b,6] Minor variations in the concentration of seed, surfactant, Ag^+ and gold in the growth solution may lead to nanorods of different aspect ratio or to anisotropic nano-objects with different shapes. Beside few other shorter chain surfactants with the same quaternary ammonium head[7a] as CTAB, and similar cetyl surfactants with tributyl or tripropyl quaternary ammonium heads (Br^- as counter anion),[7b] no other amphiphile has been reported to promote the growth of anisotropic gold nano-objects. We have discovered a new seed-growth synthesis by replacing CTAB with laurylsulfobetaine (LSB, *N*-dodecyl-*N*′, *N*′′- dimethyl-3-ammonio-1-propanesulfonate, see ESI S6 for formula†), leading to branched Au NP whose LSPR position is controlled by LSB concentration. LSB is a zwitterionic surfactant with 2 mM critical micelle concentration.[8] In a typical preparation a gold NP seed solution is prepared by mixing 5 mL of 5×10^{-4} M $HAuCl_4{\cdot}2H_2O$ with 5 mL 0.20 M LSB in water, and by adding 600 μL of $NaBH_4$ 0.010 M, obtaining the typical brownish colour of a few-nm sized Au NP dispersion. Transmission electron microscopy (TEM) reveals the formation of spherical NPs with $d < 4$ nm (see ESI†). Growth solutions were prepared with 5 mL of LSB of varying concentration (0.2–0.6 M), 180–550 μL 0.004 M $AgNO_3$, 5 mL 0.001 M $HAuCl_4{\cdot}2H_2O$ and 70 μL ascorbic acid. After the addition of ascorbic acid, the solution became colorless. Addition of 12 μL of seed solution made the growth solution to become first grey, then to develop a deep blue-violet color. It is important to stress that we have used concentrations and volumes identical to those that with 0.2 M CTAB (instead of LSB) were reported to produce NR (AR < 4.5, LSPR < 850 nm).[4b]

Observation of UV-Vis spectra revealed the growth of a major band at λ_{max} 700–1100 nm ("long" band), whose exact position depends on LSB concentration, of a less intense band at 520–530 nm ("short" band) and of a third band with λ_{max} positioned in the 650–750 nm range, depending on LSB concentration ("intermediate" band). The latter appears as a single peak or a shoulder, depending on the position of the long band. Moreover, its absorbance varied randomly from negligible to comparable to that of the long band. Attribution of the three bands was obtained by TEM. Image (i) in Fig. 1 has been taken on a dispersion from a growth solution prepared with 0.6 M LSB, featuring the full three-band profile in the UV-Vis spectrum (Fig. 2E).

Three typologies of objects are present: (**A**) nanospheres (<20 nm diameter), to which the 520–530 nm LSPR band is obviously attributed (although a contribution to this band may also be due to the transverse LSPR of the larger nano-objects); (**B**) nanostars, with large trapezoidal branches (intermediate band); (**C**) branched asymmetric NPs, with narrow, long branches (long band) of high AR (Fig. 1(iii)–(v) display isolated images of the three typologies). Image (ii) has been taken on a dispersion obtained with a 0.5 M growth solution displaying a negligible intermediate band in the UV-Vis spectrum (Fig. 2D): in this case objects of typology **B** are almost absent (~2%; type **A** 28%, type **C** 70%). For anisotropic branched NPs, the LSPR position has been reported to be proportional to the length/base ratio of

[a] *Dipartimento di Chimica Generale, Università di Pavia, viale Taramelli 12, 27100 Pavia, Italy. E-mail: piersandro.pallavicini@unipv.it; Fax: +39 0382 528544; Tel: +39 0382 987336*
[b] *Dipartimento di Fisica G. Occhialini, Università Milano Bicocca, Piazza della Scienza 3, 20126 Milano, Italy*
[c] *Istituto Italiano di Tecnologia, via Morego 30, 16163 Genova, Italy*

† Electronic supplementary information (ESI) available: TEM images of seeds and of the obtained nano-objects at various LSB concentration; DLS correlation functions and distributions of sizes; details on PEG-SH coating procedure and of the calculation of the grafted PEG-SH quantity; Full HRTEM images; ED image; TGA and SEM EDS analysis; calculation of yields; % distribution of the three typologies. See DOI: 10.1039/c0cc02682d

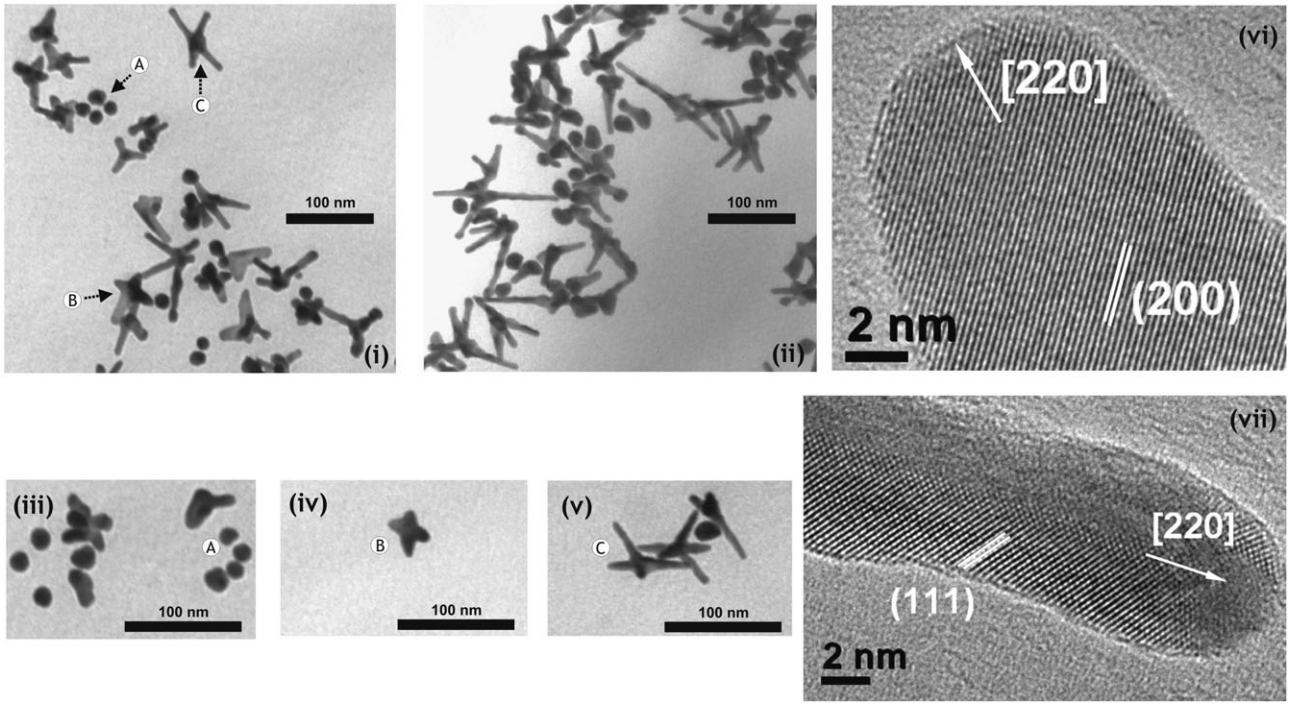

Fig. 1 TEM images (i): obtained from a growth solution prepared with 0.6 M LSB, with a three band absorption spectrum (Fig. 2B, spectrum e); (ii): obtained from a growth solution 0.5 M LSB, with a negligible intermediate band (Fig. 2B spectrum d); (iii) nanospheres (from a 0.6 M LSB growth solution), 30% magnified; (iv) nanostar, 30% magnified; (v) branched asymmetric nano-objects 30% magnified (both from a 0.2 M LSB growth solution). (vi) and (vii): HR TEM images (ESI: full and additional images†); (vi) is a detail of a monocrystalline nanostar (typology **B**), parallel white lines evidence lattice planes with 0.204 nm distance; (vii) is a detail of a twinned asymmetric branched NP (typology **C**), parallel white lines evidence lattice planes with 0.235 nm distance. Arrows evidence growth directions.

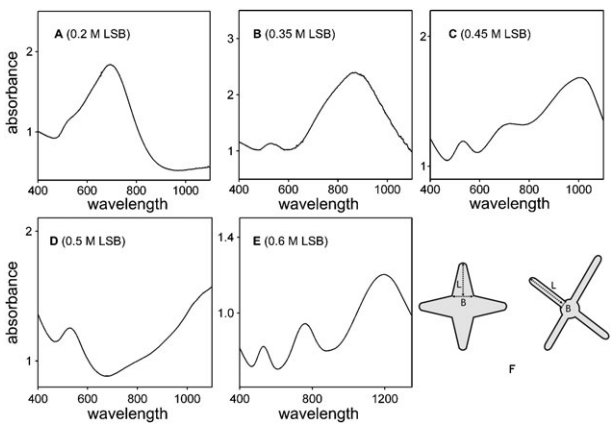

Fig. 2 A-E: UV-VIS spectra of the nano-objects dispersions from growth solutions made with 0.2-0.6 M LSB. The relevant LSB concentrations are shown in the panels. All spectra except E are in the 300-1100 nm range. Spectrum D has a negligible intermediate band (see also ESI S10†). F represents the ideal shape features of the nano-objects (L = branch length, B = branch base width).

the branches (L/B, Fig. 2F)[3b] or, similarly, to the length/aperture angle ratio of the branches,[3c] while it is independent on the number of branches grown on the core.[3c] This agrees with the assignment of the intermediate band to the **B** typology objects (nanostars) and of the long band to the **C** typology objects. Population (see also ESI, S5†) is typically ~10% type **A**, 30–50% type **B**, 40–60% type **C**. The yield, calculated as total Au found in the nano-objects mixture with respect to total starting Au, is typically 29–55% (ESI, S7†). The position of the long LSPR band scales with the LSB concentration used to prepare the growth solution. Fig. 2A–E displays spectra obtained with 0.2–0.6 M LSB. The "long" LSPR maximum position depends linearly on the surfactant concentration (Fig. S11A, ESI†). A plot of the ratio of the length to base width (L/B) of the branches, calculated from TEM images, shows a similar dependence on the LSB concentration for the type **C** objects (Fig. S11B, ESI†).

The L/B ratio for type **B** objects has been calculated only on images from 0.2 to 0.45 M solutions, as with higher LSB concentrations the tendency of the nano-objects to crop in dense assemblies on the TEM grids prevented graphical evaluations on the star nano-objects, see ESI.† In each synthesis a ~3 units lower L/B ratio is found for the **B** population with respect to type **C** objects, with a slight tendency to increase with LSB concentration (Fig. 11B, ESI†). Dynamic light scattering (DLS) measurements substantially validate this picture. Contribution to scattering of LSB micelles is negligible (pure LSB solutions revealed spherical micelles with diameter increasing from 3.2 ± 0.24 nm to 6.0 ± 0.4 nm on increasing concentration from 0.2 to 0.6 M, see also ESI†). In any dispersion small, spherical objects are observed (type **A**, hydrodynamic radius, r_H, 6–10 nm) together with larger ones. The latter display both a rotational and a translational decay of the correlation function (ESI†), whose values allow to evaluate the amount of depolarized scattering to the correlation function.[9] The nanostars and the branched asymmetric NP (*i.e.* type **B** and **C**) do not give separate

contributions in the DLS autocorrelation functions, meaning that they have similar r_H. Though the average r_H is in fact 23 ± 4 nm, independent of the LSB concentration, the ratio of the rotational to the translational scattering amplitude (Rsc/Tsc) does increase linearly with the LSB concentration (Fig. S11C, ESI†). Although this cannot be put in direct relation with the L/B ratio, it indicates that the increase of surfactant concentration promotes the formation of objects with increasing shape anisotropy (see also ESI†).

The structural details, the crystal structure growth directions and the crystallinity of type **B** and **C** objects have been further investigated by High Resolution TEM. The products are crystalline with fcc structure (see also electron diffraction, ESI S8†). All the examined type **B** objects are monocrystalline with 4 or 5 branches (in many examined object a sixth branch may be hidden behind the structure, see ESI, Fig. S9a–c†). Branches are grown along the [220] and [002] directions, as shown in Fig. 1(vi). Type **C** objects, see Fig. 1(vii) and ESI,† are always twinned crystals with {111} contact planes, with branches grown along the [220] or [002] directions. Reasoning with the widely accepted model developed for the anisotropic growth of nanorods,[5] both for type **B** and **C** objects the {111} faces must be selectively protected by LSB adsorption, while branches growth takes place by Au deposition on the free {220} and {002} faces. LSB has been reported to adsorb and form stable aggregates on the {111} face of bulk gold electrodes.[10] Moreover, it should be remembered that the formation of an anionic layer on the surface of any Au nano-object is necessary for its stabilization (even in the case of cationic surfactants as stabilizers).[11] In syntheses identical to ours, that use CTAB instead of LSB, Br^- is $\sim$0.2 M and nanorods are obtained.[4b] In our synthetic conditions there are no anions in such huge concentration. We have separated our products by ultracentrifugation and analyzed the composition by means of electron dispersion microanalysis (see ESI S7†), finding negligible traces of chloride (available in solution from $AuCl_4^-$ reduction, maximum possible concentration 0.002 M). We may thus hypothesize that the anionic sulfate moiety of LSB preferentially interacts with the {111} face of the growing Au objects (where it forms a bilayer by interdigitation of the dodecyl chains). This is also supported by considering that the Au–Au distance in {111} is 2.35 Å. This matches very well with the O–O bite length of 2.37 Å (calculated for an alkyl-SO_3^- moiety, ESI S6†), differently from the Au–Au distance in the {220} face, that is 1.44 Å.

Although the reaction of Br^- to form solid AgBr in the CTAB-driven synthesis of NR has been invocated[6] to justify the necessity of small quantities of Ag^+ in the growth solution to obtain NR with high AR, the role of Ag^+ remains largely unclear and it is still discussed in the literature. Br^- is absent using LSB, and also AgCl is not found in the products. However, Ag^+ is necessary also in our case: if not added in the growth solution, only nanospheres are obtained. Variation of Ag^+ quantity indicates that it must be proportional to LSB molarity, with an optimal [Ag^+]/[LSB] ratio of $\sim 7 \times 10^{-4}$ for the highest L/B values.

In this communication we evidence that the novelty brought by using LSB leads to branched nano-objects with very high AR (L/B) of the branches, which is unusual for similar objects obtained with CTAB. Consequently, LSPR is significantly near-IR shifted. We also want to stress an advancement in the underrated problem of appending R–SH functions on nano-objects prepared with seed-growth methods. When CTAB is used as stabilizer, under smooth reaction conditions (water, RT, one centrifugation/redispersion cycle) R–SH is grafted only to the two short tips of a NR.[12] With our products the existence of more tips increases the available points per object where grafting can be carried on. Moreover, the different nature of LSB (neutral, although zwitterionic) with respect to CTAB (cationic) may also allow the easier R–SH adsorption on the whole nano-object surface. As a matter of fact, abundant R–SH deposition is found (see ESI S4†).

Financial support from Fondazione Cariplo (Bandi Chiusi 2007, "Superfici vetrose a azione antimicrobica basata sul rilascio modulato e controllato di cationi metallici") is gratefully acknowledged.

Notes and references

1 (*a*) C. Burda, X. Chen, R. Narayanan and M. A. El-Sayed, *Chem. Rev.*, 2005, **105**, 1025; (*b*) A. Gole and C. J. Murphy, *Chem. Mater.*, 2004, **16**, 3633–3640; (*c*) V. Sharma, K. Park and M. Srinivasarao, *Mater. Sci. Eng., R*, 2009, **65**, 1–38; (*d*) Y. Yu, S. Chang, C. Lee and C. R. C. Wang, *J. Phys. Chem. B*, 1997, **101**, 6661.

2 (*a*) C. J. Murphy, A. Gole, J. W. Stone, P. N. Sisco, A. M. Alkilany, E. C. Goldsmith and S. C. Baxter, *Acc. Chem. Res.*, 2008, **41**, 1721–1730; (*b*) X. Huang, S. Neretina and M. A. El-Sayed, *Adv. Mater.*, 2009, **21**, 4880–4910.

3 (*a*) M. Yamamoto, Y. Kashiwagi, T. Sakata, H. Mori and M. Nakamoto, *Chem. Mater.*, 2005, **17**, 5391–5393; (*b*) G. C. Khoury and T. Vo-Dinh, *J. Phys. Chem. C*, 2008, **112**, 18849–18859; (*c*) P. S. Kumar, I. Pastoriza-Santos, B. Rodriguez-Gonzalez, F. J. Garcia de Abajo and L. M. Liz-Marzan, *Nanotechnology*, 2008, **19**, 015606; (*d*) S. Chen, Z. Lin Wang, J. Ballato, S. H. Foulger and D. L. Carroll, *J. Am. Chem. Soc.*, 2003, **125**, 16186–16187; (*e*) T. K. Sau and C. J. Murphy, *J. Am. Chem. Soc.*, 2004, **126**, 8648–8649; (*f*) E. Hao, R. C. Bailey, G. C. Schatz, J. T. Hupp and S. Li, *Nano Lett.*, 2004, **4**, 327–330; (*g*) W. Ahmed, E. S. Kooij, A. van Silfhout and B. Poelsema, *Nanotechnology*, 2010, **21**, 125605; (*h*) G. Kawamura and N. Nogami, *J. Cryst. Growth*, 2009, **311**, 4462–4466; (*i*) G. Kawamura, Y. Yang, K. Fukuda and M. Nogami, *Mater. Chem. Phys.*, 2009, **115**, 229–234; (*j*) C. L. Nehl and J. H. Hafner, *J. Mater. Chem.*, 2008, **18**, 2415–2419.

4 (*a*) N. R. Jana, L. Gearheart and C. J. Murphy, *J. Phys. Chem. B*, 2001, **105**, 4065–4067; (*b*) B. Nikoobakht and M. A. El-Sayed, *Chem. Mater.*, 2003, **15**, 1957–1962.

5 C. J. Johnson, E. Dujardin, S. A. Davis, C. J. Murphy and S. J. Mann, *J. Mater. Chem.*, 2002, **12**, 1765–1770.

6 N. R. Jana, L. Gearheart and C. J. Murphy, *Adv. Mater.*, 2001, **13**, 1389–1393.

7 (*a*) J. Gao, C. M. Bender and C. J. Murphy, *Langmuir*, 2003, **19**, 9065–9070; (*b*) X. Kou, S. Zhang, C.-K. Tsung, Z. Yang, M. H. Yeung, G. D. Stucky, L. Sun, J. Wqng and C. Jan, *Chem.–Eur. J.*, 2007, **13**, 2929–2936.

8 J. G. Weers, J. F. Rathman, F. U. Axe, C. A. Crichlow, L. D. Foland, D. R. Scheuing, R. J. Wiersema and A. G. Zielske, *Langmuir*, 1991, **7**, 854.

9 B. J. Berne and R. Pecora, *Dynamic Light Scattering: With Applications to Chemistry, Biology, and Physics*, Wiley, New York, 2000.

10 S. Xu, M. Chen, E. Cholewa, G. Szymanski and J. Lipkowski, *Langmuir*, 2007, **23**, 6937–6946.

11 S. Özkar and R. G. Finke, *J. Am. Chem. Soc.*, 2002, **124**, 5796–5810.

12 (*a*) K. K. Caswell, J. N. Wilson, U. H. F. Bunz and C. J. Murphy, *J. Am. Chem. Soc.*, 2003, **125**, 13914–13915; (*b*) D. Fava, Z. Nie, M. A. Winnik and E. Kumacheva, *Adv. Mater.*, 2008, **20**, 4318–4322.